CONSERVATOIRE NATIONAL
DES ARTS ET MÉTIERS
–
ROYAL INSTITUTE
OF TECHNOLOGY

le cnam

KTH VETENSKAP OCH KONST
KTH Engineering Sciences

Centre for ECO^2 Vehicle Design

A study of tailoring acoustic porous material properties when designing lightweight multilayered vehicle panels

Eleonora Lind Nordgren

Doctoral Thesis

Stockholm, Sweden 2012
The Marcus Wallenberg Laboratory for Sound and Vibration Research
Department of Aeronautical and Vehicle Engineering

Postal address
Royal Institute of Technology
MWL/AVE
SE-100 44 Stockholm
Sweden

Visiting address
Teknikringen 8
Stockholm

Contact
Tel: +46 8 790 79 41
E-mail: eleonora@kth.se

Akademisk avhandling som med tillstånd av Kungliga Tekniska Högskolan i Stockholm framläggs till offentlig granskning för avläggande av teknologie doktorsexamen fredagen den 7:e september 2012, 14:00 i sal F3, Lindstedtsvägen 26, Kungliga Tekniska Högskolan, Stockholm.

TRITA-AVE-2012:52
ISSN-1651-7660
ISBN-978-91-7501-448-7

Abstract

The present work explores the possibilities of adapting poro-elastic lightweight acoustic materials to specific applications. More explicitly, a design approach is presented where finite element based numerical simulations are combined with optimization techniques to improve the dynamic and acoustic properties of lightweight multilayered panels containing poro-elastic acoustic materials.

The numerical models are based on Biot theory which uses equivalent fluid/solid models with macroscopic space averaged material properties to describe the physical behaviour of poro-elastic materials. To systematically identify and compare specific beneficial or unfavourable material properties, the numerical model is connected to a gradient based optimizer. As the macroscopic material parameters used in Biot theory are interrelated, they are not suitable to be used as independent design variables. Instead scaling laws are applied to connect macroscopic material properties to the underlying microscopic geometrical properties that may be altered independently.

The design approach is also combined with a structural sandwich panel mass optimization, to examine possible ways to handle the, sometimes contradicting, structural and acoustic demands. By carefully balancing structural and acoustic components, synergetic rather than contradictive effects could be achieved, resulting in multifunctional panels; hopefully making additional acoustic treatment, which may otherwise undo major parts of the weight reduction, redundant.

The results indicate a significant potential to improve the dynamic and acoustic properties of multilayered panels with a minimum of added weight and volume. The developed modelling techniques could also be implemented in future computer based design tools for lightweight vehicle panels. This would possibly enable efficient mass reduction while limiting or, perhaps, totally avoiding the negative impact on sound and vibration properties that is, otherwise, a common side effect of reducing weight, thus helping to achieve lighter and more energy efficient vehicles in the future.

Résumé

Le présent travail explore la possibilité d'adapter des matériaux poro-élastiques légers pour des applications spécifiques. En particulier, une approche de conception est présentée, combinant simulations par la méthodes des éléments finis et techniques d'optimisation, permettant ainsi d'améliorer les propriétés dynamiques et acoustiques de panneaux multicouches comprenant des matériaux poreux.

Les modèles numériques sont fondés sur la théorie de Biot qui utilise des modèles équivalents fluide/solide avec des propriétés macroscopiques spatialement homogénéisées, décrivant le comportement physique des matériaux poro-élastiques. Afin de systématiquement identifier et comparer certaines propriétés spécifiques, bénéfiques ou défavorables, le modèle numérique est connecté à un optimiseur fondé sur les gradients. Les paramètres macroscopiques utilisés dans la théorie de Biot étant liés, il ne peuvent être utilisés comme variables indépendantes. Par conséquent, des lois d'échelle sont appliquées afin de connecter les propriétés macroscopiques du matériau aux propriétés géométriques microscopiques, qui elles peuvent être modifiées indépendamment.

L'approche de conception est également combinée avec l'optimisation de la masse d'un panneau sandwich structure, afin d'examiner les possibilités de combiner exigences structurelles et acoustiques, qui peuvent être en conflit. En prenant le soin d'établir un équilibre entre composantes acoustiques et structurelles, des effets de synergie plutôt que destructifs peuvent être obtenus, donnant lieu à des panneaux multifonctionnels. Cela pourrait rendre l'ajout de traitements acoustiques redondant, qui par ailleurs annulerait tout ou partie du gain en masse obtenu par optimisation.

Les résultats indiquent un véritable potentiel d'amélioration des propriétés dynamiques et acoustiques de panneaux multi-couches, pour un ajout minimum en termes de masse et volume. La technique de modélisation développée pourrait également être implémentée au sein d'outils numériques futures pour la conception de panneaux légers de véhicules. Cela aurait le potentiel de réduire substantiellement la masse tout en limitant, voire supprimant l'impact négatif sur les propriétés acoustiques et vibratoires, pourtant une conséquence courante de la réduction de la masse, participant ainsi à l'effort de développement de véhicules futures plus légers et efficaces.

Doctoral thesis

This thesis consists of the following papers:

Paper I
E. Lind Nordgren and P. Göransson. Optimising open porous foam for acoustical and vibrational performance. *Journal of Sound and Vibration* 2010; **329**(7): pp. 753-767.

Paper II
C. J. Cameron, E. Lind Nordgren, P. Wennhage and P. Göransson. Material Property Steered Structural and Acoustic Optimization of a Multifunctional Vehicle Body Panel. Submitted and under revision.

Paper III
C. J. Cameron, E. Lind Nordgren, P. Wennhage and P. Göransson. A Design Method using Topology, Property, and Size Optimization to Balance Structural and Acoustic Performance of Sandwich Panels for Vehicle Applications. Submitted and under revision.

Paper IV
E. Lind Nordgren, P. Göransson and J.-F. Deü. Alignment of anisotropic poro-elastic layers - Sensitivity in vibroacoustic response due to angular orientation of anisotropic elastic and acoustic properties. To be submitted.

Division of Work Between the Authors

Paper I. Nordgren derived the formulations, performed the computations and wrote the paper under the supervision of Göransson.

Paper II and Paper III. The work was performed in collaboration with Cameron on combined acoustic and structural optimization, where the acoustic optimization was performed by Nordgren. The papers were written together, where Nordgren wrote the parts regarding the acoustics in the introduction, optimization and results. Cameron did the same for the structural parts. Conclusions were derived by the aforementioned authors together with supervisors Wennhage and Göransson and written by Nordgren and Cameron together.

Paper IV. Nordgren derived the formulations, performed the computations and wrote the paper under the supervision of Göransson and Deü.

Acknowledgments

The work presented in this thesis has been carried out within in the Centre for ECO^2 Vehicle Design at the Marcus Wallenberg Laboratory (MWL) and within the Smart Structures network at Laboratoire de Mécanique des Structures et des Systèmes Couplés (LMSSC) at the Conservatoire National des Arts et Métiers (CNAM). The financial support is gratefully acknowledged.

First I would like to thank my supervisor, Peter Göransson, for giving me the opportunity to take on this inspiring, gratifying and frustrating challenge, and for your support and guidance along the way. Your confidence in me and this project as well as your great knowledge and devotion to the subject has been invaluable.

Further I would like to thank my other supervisor, Roger Ohayon at LMSSC, and my assistant supervisors, Nils-Erik Hörlin at MWL and Jean-François Deü at LMSSC, for taking the time to answer my many questions varying from theoretical aspects of numerical simulations and computational issues to practical matters related to this joint Swedish-French PhD. Also, I would like to thank the administrative staff for their patience when handling all the different issues of administrative matter.

To Christopher J. Cameron, with whom a substantial part of this work was carried out, thank you for the interesting discussions and the insights in a different research area. The collaborative work has definitely helped me become a more versatile researcher.

To my colleges I would like to extend my thanks for creating such a stimulating and open-minded work environment, especially to Eskil Lindberg for being a great office mate and for sharing your honest and down-to-earth views in all sorts of questions.

I am also grateful to all of my friends and family for making my life so much more enjoyable. Special thanks to my beloved Mamma, Pappa, Syster, Bror and Farmor for their encouragement and genuine love and care throughout my life. And yes, I am now just about finished with "school" ...

Finally, MIKAEL, thank you! Completing this thesis would not have been possible without your love and support. You are truly wonderful! ♡

Contents

Part I

Overview and Summary

Chapter 1

Introduction

The environmental impact caused by human activities in general, has become an increasingly important issue on a global scale. Major parts of the discussion today regard global warming, for which emissions of carbon dioxide and other green house gases are considered responsible. In Sweden approximately 26% of the energy consumption is due to the transport industry, and according to Åkerman and Höjer [24] this is already too much. In order to achieve a sustainable environmental impact the energy used for transport would actually need to be decreased by 60% until year 2050. This can only be done by far reaching changes in transport patterns combined with a significant reduction of energy intensity of transport. Many aspects of a vehicle have to be considered in order to improve the energy efficiency. Apart from the drive line itself, rolling resistance, aerodynamic properties and overall vehicle weight are just a few of many characteristics that highly influence the total life cycle energy consumed.

Reducing the weight of a vehicle is therefore one of many strategies to reduce the fuel or energy consumption and hence achieve more effective transportations with less negative environmental impact. Concurrently, the demands on safety and comfort will not be lowered and changes made to the structure must hence strive to sustain or even improve those properties. This may be accomplished by e.g. far-reaching changes in selected materials as well as overall design, and the implementation of light and stiff multilayered and multifunctional structures (e.g. sandwich panels and sandwich composites) in industrial production has steadily increased for some time. Although, along with the introduction of new lightweight designs, increased problems with noise and vibration often follows, in particular at low frequencies. Typically, unwanted structural vibrations and noise are carried through the structure and radiate, for example, from trim surfaces inside the cabin of a vehicle. Consequently, the dynamic behaviour of such interior trim panel has a major impact on the radiated noise and hence the interior noise levels.

Adding flexible poro-elastic and visco-elastic materials is an often used method to improve noise, vibration and harshness (NVH) comfort in vehicles under such circumstances when major modifications of the interior trim panels are not possible. However, adding material is problematic in view of the goal of reducing weight. It also

adds to the overall cost, material and assembly, and may also take up space that might otherwise come to the benefit of the user. It would of course be highly sought after to include acoustic and dynamic requirements in the original design of the panel or, as a second option, to assure that the best possible performance per added weight, cost and volume of any latterly added treatment is achieved.

A common way to enhance the performance of an acoustic trim panel is to combine different poro-elastic and visco-elastic materials into several layers with different physical and mechanical properties, such as damping, elasticity, viscosity and density. Determining which materials to combine and what properties to look for in each individual layer in order to achieve satisfactory result, is today an expensive and time consuming task that requires knowledge of previously successful combinations, engineering experience as well as extensive testing. Clearly there is a need for computational tools that are able to predict and optimize the behaviour of such multilayered structures.

This work is an initial attempt to demonstrate the possibilities of adapting porous materials to specific purposes. Done correctly, it can potentially generate considerable improvements in NVH comfort with a minimum of added volume and weight.

Chapter 2

Describing and designing porous media

The materials treated in this work are porous materials, consisting of heterogeneous materials constituting an elastic porous framework saturated with fluid. The fluid is assumed to be interconnected throughout the media, so called open pores or open cells. The interstitial fluid, e.g. air, can move relative to the frame, thus any fluid that is enclosed in the framework is considered as part of the frame since it cannot execute relative motion. Two typical porous materials are open cell foam and fibrous material, see fig. 2.1 and 2.2. In porous foam the slender beams constituting the frame are often referred to as struts. The porosities of materials used as acoustic absorbents are normally high, above 90%, and the acoustic energy is carried both through the fluid in the pores as well as through the solid frame material. The waves are strongly coupled and propagate simultaneously along the two paths but with different phase and amplitude. The wave propagation in porous media is, in other words, a fluid-structure interaction phenomenon, occurring throughout the whole volume of material.

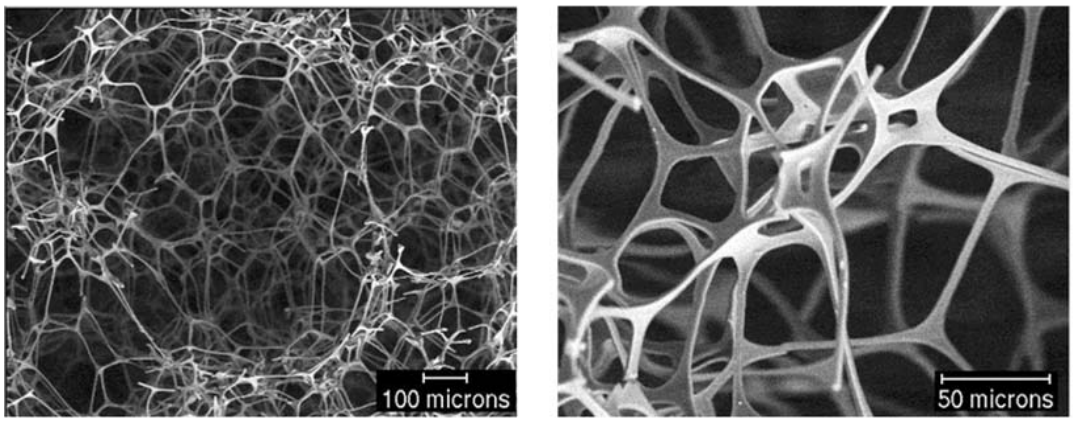

Figure 2.1: Microscopic photography of an open cell porous foam structure. Picture courtesy of Franck Paris (CTTM, France) and Luc Jaouen (luc.jaouen@matelys.com).

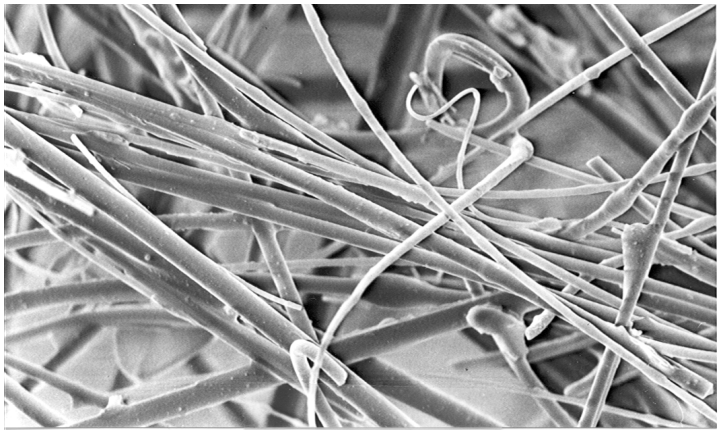

Figure 2.2: Microscopic photography of fibrous material. Picture courtesy of Rémi Guastavino (remi@kth.se).

2.1 Energy dissipation in porous media

When acoustic energy enters a porous media a proportion of the mechanical-acoustical energy will be lost, i.e. converted into heat. There are several different mechanisms that contribute to the advantageous acoustic and vibro-acoustic behaviour of porous media, some of these mechanisms will be briefly described below.

When the frame and the fluid move relative each other, viscous drag will appear at the interface, this will initiate losses in the fluid as well as in the frame. The viscous drag is assumed proportional to the relative displacement and is usually described by using a frequency dependent proportionality factor. Such factor is not only dependent on frequency, but also on, for example, the geometrical properties of the pores, the viscosity of the interstitial fluid and the contact area between the frame and the fluid. At low frequencies the viscous boundary layer at the strut surface is thick relative to the pore radius and the loss of acoustic energy due to viscous dissipation is significant. While at higher frequencies the viscous boundary layer between the frame and the fluid, the viscous skin depth, will be much smaller than the pore radius. At such rapid oscillations the viscous dissipation is small compared to other phenomena.

The movement of fluid relative the frame will not only cause the viscous forces mentioned above. In addition to the viscous drag there are other mechanisms that cause vibro-acoustic energy losses which are proportional to the relative displacement but independent of the viscosity of the fluid. As the fluid (or frame) is forced to change direction, while moving relative to the frame (or fluid), a force normal to the direction of acceleration of one element will be applied to the other. These mechanisms, that would be present even under the assumption of an inviscid fluid, create an apparent increase of mass and are related to the geometry of the frame as well as to the relative motion.

The movement of the frame will also cause frequency dependent internal losses due to the stress-strain relaxation as the frame is deformed. Thermoelastic dissipation

is yet another source of dissipation of acoustic energy as the compressibility of the system yields an increase of temperature due to the compression and expansion cycles. At low frequencies the process is isothermal while as at high frequencies the process becomes adiabatic. In between these conditions, heat conduction among other physical phenomena will cause losses in vibro-acoustic energy.

2.2 Biot theory

The most commonly used model to describe the acoustic behaviour of porous media is attributed to Biot [5] and often referred to as the Biot theory, or sometimes as the Johnson-Champoux-Allard model of the Biot theory. Part of Biot's theory published in 1956 is similar to the contemporary one presented by Zwikker and Kosten [34] with the difference that Biot also included the effects of shear stress in the elastic frame of the porous medium.

Johnson *et al.* [23] added an improved description of the viscous effects by introducing the characteristic viscous length, Λ, which takes frequency dependent viscous effects into account. Allard and Champoux [2, 9] added the characteristic thermal length, Λ', which similarly includes the effects of frequency dependent thermal losses.

Within the extended Biot theory the solid frame is modelled as an equivalent elastic solid continuum and the interstitial fluid as an equivalent compressible fluid continuum, both described by space averaged macroscopic mechanical properties common in continuum mechanics. The two separate but coupled continua are then acting and interacting while occupying the same space. The interaction between the solid and fluid phase is described through coupling parameters derived from measurable macroscopic space averaged properties. The macroscopic properties are used to calculate macroscopic space averaged quantities e.g. solid and fluid displacement, acoustic pressure, and elastic stress. One condition for the above modelling of foams is that the characteristic microscopic dimensions of the foam, e.g. pore size, are small compared to characteristic dimensions of the macroscopic behaviour. In acoustics the latter is identified as the wave length. For the models and materials investigated here, this condition is generally satisfied.

It should however be noted that the modelling of poro-elastic material as two separate, coupled continua is problematic at the boundary of the material. Studies show the homogenized properties may be quite different close to the surface of the poro-elastic material [17]. These types of boundary effect could have a not insignificant impact, especially if the depth of such boundary layer is large compared to the thickness of the porous layer.

A substantial amount of work has been done to obtain physically meaningful descriptions of the macroscopic material parameters. Especially significant for porous media are the

coupling parameters which may be defined in different ways. Within the Johnson-Champoux-Allard model they are mostly described as:

- *Porosity*, ϕ [1], defined as the volume fraction of fluid content in the porous media, $0 < \phi < 1$. For materials used in acoustic applications the porosity is normally larger than 0.95.

- *Tortuosity*, α_∞ [1], defined as the fraction between mean microscopic fluid velocity squared and the mean macroscopic fluid velocity squared averaged over a volume under the assumption of zero viscosity. In practice it compares the length of the path the fluid travels in the porous media on microscopic level with the length of the path on a macroscopic level, implying that $\alpha_\infty \geq 1$. For open porous media with high porosity the tortuosity is often close to one, typically 1.05.

- *Static flow resistivity*, σ^{static} [Nsm^{-4}], defined as the pressure difference over flow velocity per unit length. The flow resistivity is dependent of many different physical properties in the porous media, among them the surface viscosity between the frame and the microscopic geometry of the porous media. This parameter may be measured or theoretically deduced from e.g. Stokes simulations given a certain microstructural geometry.

- *Viscous characteristic length*, Λ [m], helps to improve the estimation when dissipation effects due to viscous losses at the pore walls need to be taken into account. When the pores are small compared to the viscous skin depth the viscous dissipation effects cannot be neglected. The viscous characteristic length provides possibilities for modifications that give better frequency dependent representation of the viscous losses.

- *Thermal characteristic length*, Λ' [m], takes into account the thermal exchange between the frame and the fluid at the boundary, in analogy with the viscous characteristic length, hence similarly provides adjustments for the frequency dependent thermal fluid-structure interactions.

An important part for increased understanding of porous materials is the experimental work carried out to characterize different materials and obtain the macroscopic material parameters needed. There are also still several not fully understood physical aspects of porous materials, for example the influence of static compression, strain or other deformations on the material properties [13] or the changes of elastic moduli at the boundary region of porous foam samples [17]. Naturally the work to obtain experimental data are closely connected to the work of developing mathematical models used to describe these complex materials and their behaviour.

2.2.1 Governing equations

The Biot theory is a Lagrangian model where the stress-strain relations are derived from potential energy deformation. While Biot theory, in practice, often is used in its isotropic form, the anisotropic form of the governing equations, similar to what has been previously stated by Biot [7], Biot and Willis [8] and Allard [1] will be given here. This overview of the governing equations is in no way complete and should be considered as a short summary of the very extensive work that has been previously accomplished in the field of porous materials. The interested reader is referred to the original work for details.

The notations used is explained when introduced and also summarized in Chapter 6, except for the following regarding tensor notation. The component ordinal number in a Cartesian co-ordinate system, e.g. $i = 1, 2, 3$ is noted i, j, k. Partial derivates with respect to x_i is written $(.)_{,i} = \partial(.)/\partial x_i$. Kronecker's delta is δ_{ij}. Also, Cartesian tensor notation with Einstein's summation convention is used, i.e. repeated indices imply a summation of these terms.

Momentum equations

Assuming time harmonic motion at circular frequency ω, the (frequency domain) momentum equations for the solid frame and the fluid respectively may be written as

$$\sigma^{\mathrm{s}}_{ij,j} = -\omega^2 \tilde{\rho}^{11}_{ij} u^{\mathrm{s}}_j - \omega^2 \tilde{\rho}^{12}_{ij} u^{\mathrm{f}}_j \tag{2.1}$$

and

$$\sigma^{\mathrm{f}}_{ij,j} = -\omega^2 \tilde{\rho}^{12}_{ij} u^{\mathrm{s}}_j - \omega^2 \tilde{\rho}^{22}_{ij} u^{\mathrm{f}}_j \tag{2.2}$$

where σ^{s}_{ij} and σ^{f}_{ij} are the Cauchy stress tensors for the frame and the fluid respectively while u^{s}_j and u^{f}_j are the frame and fluid displacements. The equivalent density tensors, $\tilde{\rho}^{11}_{ij}$, $\tilde{\rho}^{12}_{ij}$ and $\tilde{\rho}^{22}_{ij}$ are anisotropic generalizations of those used by Allard [1] and may be defined as

$$\tilde{\rho}^{11}_{ij} = \rho_1 \delta_{ij} + \rho^{\mathrm{a}}_{ij} - \frac{\mathrm{i}}{\omega} b_{ij}, \tag{2.3}$$

$$\tilde{\rho}^{12}_{ij} = -\rho^{\mathrm{a}}_{ij} - \frac{\mathrm{i}}{\omega} b_{ij}, \tag{2.4}$$

$$\tilde{\rho}^{22}_{ij} = \phi \rho_0 \delta_{ij} + \rho^{\mathrm{a}}_{ij} - \frac{\mathrm{i}}{\omega} b_{ij}, \tag{2.5}$$

where

$$\rho_{ij}^{\mathrm{a}} = \phi\rho_0 \left(\alpha_{ij} - \delta_{ij}\right) \tag{2.6}$$

with ρ_0 as the ambient fluid density and ρ_1 as the bulk density of the porous material and α_{ij} is the tortuosity tensor. ρ_{ij}^{a} is an inertial coupling coefficient that represents the apparent increase of mass due to tortuosity. The viscous drag tensor b_{ij} accounts for the viscous body forces between the solid and the fluid phase and is here defined as established by Johnson *et al.* [23].

$$b_{ij} = \phi^2 \sigma_{ij}^{\mathrm{static}} B_{ij}\left(\omega\right), \tag{2.7}$$

where

$$B_{ij} = \sqrt{1 + i\omega \frac{4\eta\rho_0\alpha_{ij}^2}{\phi^2(\sigma_{ij}^{\mathrm{static}})^2\Lambda_{ij}^2}} \tag{2.8}$$

with η being the ambient fluid viscosity.

Constitutive equations

The two constitutive equations may be defined as

$$\sigma_{ij}^{\mathrm{s}} = C_{ijkl}\varepsilon_{kl} + Q_{ij}\theta^{\mathrm{f}} \tag{2.9}$$

and

$$\sigma_{ij}^{\mathrm{f}} = Q_{kl}\varepsilon_{kl}\delta_{ij} + R\theta^{\mathrm{f}}\delta_{ij} \tag{2.10}$$

where C_{ijkl} is the solid frame Hooke's tensor, the fluid dilatation is given by the divergence of the fluid displacement

$$\theta^{\mathrm{f}} = u_{k,k}^{\mathrm{f}} \tag{2.11}$$

and the solid frame strain is given by the Cauchy strain tensor

$$\varepsilon_{kl} = \frac{1}{2}\left(u_{k,l}^{\mathrm{s}} + u_{l,k}^{\mathrm{s}}\right) \tag{2.12}$$

The two material tensors, R and Q_{ij} are defined as

$$R = \frac{\phi^2 K_s}{1 - \phi - K_s C_{ijkl} d_{ij} d_{kl} + \phi K_s / K_f} \tag{2.13}$$

$$Q_{ij} = \left[(1-\phi) - C_{ijkl} d_{kl}\right] \frac{R}{\phi} = \frac{\left[(1-\phi) - C_{ijkl} d_{kl}\right] \phi K_s}{1 - \phi - K_s C_{ijkl} d_{ij} d_{kl} + \phi K_s / K_f} \tag{2.14}$$

where K_s and K_f are the frame and fluid bulk modulus and d_{ij} is the unjacketed compressibility compliance tensor where K_f is obtained using the model by Lafarge *et al.* [26]. As the fluid itself is assumed to be isotropic, R is a scalar quantity. The dilatational coupling Q_{ij} is, however, a second order tensor due to the assumed elastic anisotropy.

Often in practice and also in this work the fluid displacement field is not used as dependent variable. Instead the fluid Cauchy stress tensor is replaced by the pore pressure, which is a scalar unit, $\sigma^{\mathrm{f}}_{ij} = -\phi p \delta_{ij}$, this allows for a reduction of the number of dependent variables from six to four.

2.2.2 Matrix representation of material parameters

The elastic properties of the solid frame of the porous material may be described using the solid frame Hooke's matrix, equivalent to the Hooke's tensor C_{ijkl} used previously. The Hooke's matrix is a 6×6 matrix and for isotropic materials it consists of only two independent parameters:

$$\mathbf{C} = \frac{E}{(1+\nu)(1-2\nu)} \begin{bmatrix} 1-\nu & \nu & \nu & 0 & 0 & 0 \\ & 1-\nu & \nu & 0 & 0 & 0 \\ & & 1-\nu & 0 & 0 & 0 \\ & & & \frac{1-2\nu}{2} & 0 & 0 \\ symm. & & & & \frac{1-2\nu}{2} & 0 \\ & & & & & \frac{1-2\nu}{2} \end{bmatrix} \tag{2.15}$$

where E is the Young's modulus and ν is Poisson's ratio. Anisotropic materials have many different types of anisotropy, three of which will be briefly described here.

1. *Transversely isotropic* materials have equal material properties in two of its principal direction but different ones in the third direction normal to the plane of isotropy. A typical transversely isotropic material is a fibrous material, and describing it

requires up to five independent parameters.

$$\mathbf{C} = \begin{bmatrix} C_{11} & C_{12} & C_{13} & 0 & 0 & 0 \\ & C_{11} & C_{13} & 0 & 0 & 0 \\ & & C_{33} & 0 & 0 & 0 \\ & & & C_{44} & 0 & 0 \\ symm. & & & & C_{44} & 0 \\ & & & & & \frac{1}{2}(C_{11} - C_{12}) \end{bmatrix} \tag{2.16}$$

2. *Orthotropic* materials have three axes which are mutually orthogonal and their mechanical properties are, in general, different in each direction. Further, there exists some orthogonal principal directions where there is no coupling between dilatation and shear. Many acoustic foam materials show tendencies toward orthotropic behaviour and describing them then requires at the most nine different material parameters.

$$\mathbf{C} = \begin{bmatrix} C_{11} & C_{12} & C_{13} & 0 & 0 & 0 \\ & C_{22} & C_{23} & 0 & 0 & 0 \\ & & C_{33} & 0 & 0 & 0 \\ & & & C_{44} & 0 & 0 \\ symm. & & & & C_{55} & 0 \\ & & & & & C_{66} \end{bmatrix} \tag{2.17}$$

3. *Fully anisotropic* materials may have different material properties in every direction and the principal directions are not necessary orthogonal, implying that e.g. bending in one direction may induce twisting in another, or a compressional stress may induce shear stresses. This is the most general material description, however not often used as describing it requires up to 21 independent parameters.

$$\mathbf{C} = \begin{bmatrix} C_{11} & C_{12} & C_{13} & C_{14} & C_{15} & C_{16} \\ & C_{22} & C_{23} & C_{24} & C_{25} & C_{26} \\ & & C_{33} & C_{34} & C_{35} & C_{36} \\ & & & C_{44} & C_{45} & C_{46} \\ symm. & & & & C_{55} & C_{56} \\ & & & & & C_{66} \end{bmatrix} \tag{2.18}$$

Other material properties such as tortuosity, static flow resistivity and viscous characteristic length would instead be described with a 3×3 matrix where the number of independent parameters required would vary between one, for an isotropic material, up to six for a fully anisotropic material.

1. *Isotropic*

$$\mathbf{S} = \begin{bmatrix} S_1 & 0 & 0 \\ & S_1 & 0 \\ symm. & & S_1 \end{bmatrix} \tag{2.19}$$

2. *Transversely isotropic*

$$\mathbf{S} = \begin{bmatrix} S_1 & 0 & 0 \\ & S_1 & 0 \\ symm. & & S_3 \end{bmatrix} \tag{2.20}$$

3. *Orthotropic*

$$\mathbf{S} = \begin{bmatrix} S_1 & 0 & 0 \\ & S_2 & 0 \\ symm. & & S_3 \end{bmatrix} \tag{2.21}$$

4. *Fully anisotropic*

$$\mathbf{S} = \begin{bmatrix} S_{11} & S_{12} & S_{13} \\ & S_{22} & S_{23} \\ symm. & & S_{33} \end{bmatrix} \tag{2.22}$$

For most anisotropic porous materials the material parameter matrices are to a great part unknown and the question of how to effectively measure or otherwise retrieve these parameters is still an open issue. Many of the well established techniques used today measure only the isotropic equivalent of the anisotropic properties. The ongoing work of developing adequate measurement techniques to fully characterize anisotropic porous media is not at all a trivial task. The anisotropy of a porous material does, however, have an impact on the space averaged macroscopic material properties and the acoustic behaviour of the porous material [25]. The ongoing research are focused on new measurement techniques [17] as well as studies of anisotropic microstructural geometries [21, 22, 29]. Further it should be emphasized that the principal directions of the different macroscopic material properties does not necessarily line up with each other or the main directions in a geometrical sense, they may very well require different local coordinate systems to be accurately modelled [16, 28, 31].

2.2.3 Isotropic versus anisotropic modelling

The vast majority of previously published work involving and developing Biot theory concerns only isotropic modelling and therefore the isotropic models today have several improvements that are not readily transferable to an anisotropic description. As an example, the isotropic stress-strain relations may be extended to include also the frequency dependent internal losses due to the movements in the frame. These may be modelled using the augmented Hooke's law (AHL), proposed by Dovstam [12], which is based on work from e.g. Biot [6] and Lesieutre [27]. In brief the internal losses are modelled adding frequency dependent, complex valued terms, to the classic material

modulus matrix of Hooke's generalized law. This augmented Hooke's law is today not implemented in anisotropic Biot models as several unknowns regarding the damping behaviour and its principal directions still remain.

In addition the material parameters needed to describe anisotropic materials are not easy to obtain and many questions remain regarding their principal directions. This emphasizes the need to further develop accurate measurement techniques in order to obtain information regarding the physical behaviour of anisotropic materials. These are all issues for ongoing research.

Therefore, when modelling porous materials, the choice between using isotropic or anisotropic models is dependent on e.g. the accuracy needed, the type of porous material to be modelled, the structure in which it is implemented, and also whether or not the anisotropic material parameters are known or may be obtained.

2.3 FE-modelling

Analytical solutions to Biot's equations exists only for a few special cases where the equation set-ups may be reduced to one dimensional problems, e.g. infinite plane, spherical, and infinite cylinder problems. For most applications of interest the complexity of the problem requires some kind of numerical solution that can handle complex geometries, finite sizes, non-uniform distribution of boundary conditions and loads, as well as the coupling to other porous, solid or fluid components. These issues and several more have been addressed for both the isotropic as well as the anisotropic cases in previous works by Hörlin and Göransson [19], Hörlin [18] and Hörlin *et al.* [20] where three-dimensional hp-based [1] finite element solutions have been developed and evaluated. To formulate finite element solutions to the coupled partial differential equations describing the behaviour of a system, a weak form of the partial differential equations, including boundary conditions, had to be stated. Hörlin evaluated different weak formulations, among them a mixed displacement-pressure formulation for isotropic porous materials as it was proposed by Atalla *et al.* [3, 4]. Later on the mixed displacement-pressure formulation was extended by Hörlin and Göransson [19] to include also anisotropic materials. This formulation uses the frame displacement as the primary variable describing the motion of the frame, and the fluid pressure as the primary variable describing the fluid, i.e. (u^s, p)-formulation, instead of the more common weak formulations which use frame and fluid displacement as primary variables, (u^s, u^f)-formulations. The latter has been shown to require cumbersome calculations when used in large finite element systems. The (u^s, p)-formulation as proposed by Atalla *et al.* [4] is considered as accurate as the classical (u^s, u^f)-formulation with the advantage that it is the better choice with respect to the computational effort required to achieve the wanted accuracy. It describes the porous material with a minimum of dependent

[1] Convergence is achieved by refining the mesh and/or increasing the approximation order.

field variables and it also couples two open pore components, and also an open pore component to a solid one, without any additional coupling integrals, as long as the solid parts are attached to each other. However, couplings between porous components and fluids require coupling integrals to be used. This proposed mixed displacement pressure formulation is underpinning the current work of studying the potential improvements of adapting porous materials to specific applications.

2.4 Correlations between macroscopic and microscopic properties

As stated previously, porous materials are described using the macroscopic space averaged properties, of which several are presented in the equations above. These macroscopic properties are naturally dependent on the microscopic geometrical properties of the frame as well as of the frame material itself. Examples of such geometrical, microscopic properties are the size and shape of the pores, and the cross section and thickness of the struts, or fibres, in the open porous material. Microscopic properties like these will, in combination with material choices, govern the thermal, elastic, viscoelastic, mechanical and acoustic behaviour of the porous material. Hence, the macroscopic properties can not be regarded as independent of one another and are therefore unsuitable as variables in an optimization problem. Instead, the aim in the current work has been to use scaling laws that relate the macroscopic properties to the underlying microscopic properties. Such scaling laws should preferably describe the macroscopic properties of the porous material as being continuously and systematically dependent on the micro-structural mechanical properties, allowing for the optimization to focus directly to the microscopic properties. Several researchers have made contributions in developing mathematical formulations of the relations between different material properties. Assuming an open cell foam structure with high porosity, where the strut material is significantly heavier than the interstitial fluid, the approach taken by Gibson and Ashby [14] may then provide significant guidance in understanding the mechanical behaviour of such a foam. Gibson and Ashby view the cellular structure as vertices joined by edges. A very simple configuration would be a cubic cell shape where adjoining cells are staggered so that their members meet at the mid points, but the reasoning is just as valid for more complex cell structures such as e.g. rhombic dodecahedra or tetrakaidecahedra, fig. 2.3. The last cell structure, tetrakaidecahedra, also referred to as a Kelvin cell, is a common choice because it has an average number of edges per face, and of faces per cell, which seems to correspond well to some observations, but the matter would need further investigation [14, 30]. Recent studies [11] show that such scaling laws, although based on simplified cell structures and possibly different implicit assumptions that may not be completely fulfilled, still give a fairly satisfactory prediction.

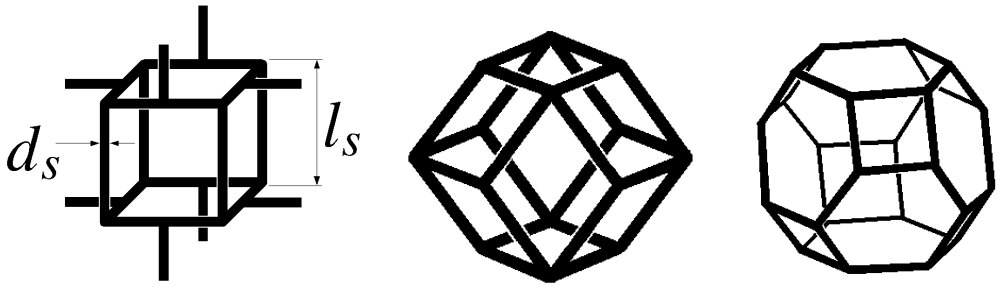

(a) cubic cell (b) rhombic dodecahedra (c) tetrakaidecahedra

Figure 2.3: Examples of theoretical cell shapes according to Gibson and Ashby.

Assuming isotropy in the cell geometry it may be shown, for all of the foam cell shapes mentioned above, that the relative density, ρ^*, for cellular foams is proportional to the length and the thickness of the struts, l_s and d_s respectively.

$$\frac{\rho^*}{\rho_s} = C^\rho \left(\frac{d_s}{l_s}\right)^2 \tag{2.23}$$

where C^ρ is a constant dependent on the cell shape and strut cross section shape, but close to unity for an open cell foam with fairly complex cell shapes. ρ_s is the frame material density. Assuming knowledge of a reference foam, denoted $(.)_{ref}$, which is scaled but still keeping its general cell and strut shape, the relative density may be expressed as

$$\rho^* = \rho^*_{ref} \left(\frac{d_s}{d_{ref}}\right)^2 \left(\frac{l_{ref}}{l_s}\right)^2 \tag{2.24}$$

The assumption that the strut material is significantly heavier than the interstitial fluid allows for the porosity to be expressed as

$$\phi = 1 - \frac{\rho^*}{\rho_s} \tag{2.25}$$

To model the variation of the Young's modulus with the microscopic properties, the struts are assumed to deform primarily in bending. Additionally, small deformations and linearly elastic behaviour of the strut material is also assumed. The deformation on a macroscopic level can be coupled to the deformation of the struts in a cubic cell by applying mechanical laws of deformation of beams. If the Young's modulus of the foam is calculated as the deflection of a beam with length l_s loaded at the midpoint by the force F, the deflection, δ, is proportional to Fl_s^3/E_sI, where E_s is the Young's modulus of the frame material and I is the moment of inertia of the strut shape, $I \propto d_s^4$. On a macroscopic scale the force is related to the macroscopic compressive stress, σ^*, as $F \propto \sigma^* \cdot l_s^2$ and the macroscopic strain, ε^*, is related to the beam deflection as $\varepsilon^* \propto \delta/l_s$. It follows that the Young's modulus for the foam can be expressed as

$$E^* = \frac{\sigma^*}{\varepsilon^*} = \frac{C^{dl} E_s I}{l_s^4} \quad \rightarrow \quad \frac{E^*}{E_s} = C^{dl} \left(\frac{d_s}{l_s}\right)^4 = C^E \left(\frac{\rho^*}{\rho_s}\right)^2 \tag{2.26}$$

or when a reference material is used as

$$E^* = E^*_{ref} \left(\frac{\rho^*}{\rho^*_{ref}}\right)^2 \tag{2.27}$$

Extensive works by Allard and Champoux [2] and Allard [1] have also contributed to establishing relations between the macroscopic foam properties and the microscopic structural properties. Their work have been used by Göransson to further develop scaling laws that relates the viscous characteristic length, Λ, and the static flow resistivity, σ^{static}, to the microstructure of the foam [15]. By assuming inviscid flow around a cylinder Allard and Champoux show that if the porosity is close to one, Λ is given by

$$\Lambda = \frac{1}{2\pi L r} \tag{2.28}$$

where L is the total cylinder length per unit volume and r is the radius of the cylinder [2]. With the former assumption of cellular geometry L can be defined in terms of the porosity as $\pi r^2 L = \rho^*/\rho^s$ which allow for the viscous characteristic length to be expressed as [15]

$$\Lambda = \frac{d_s}{4(\rho^*/\rho_s)} = \frac{d_s}{4(1-\phi)} \tag{2.29}$$

To account for thermal effects the simplified assumption of $\Lambda' = 2 \cdot \Lambda$ has been made for the thermal characteristic length, Λ'. As the tortuosity for highly porous materials is very depend on the closed pore content and the materials used in this work are assumed to be only open pores, the change in tortuosity when the material properties are altered is quite small. However, a scaling law based on work by Comiti and Renaud, [10], have been implemented in Paper II and III,

$$\alpha_\infty = 1 - \frac{1 - \alpha_{\infty ref}}{\ln(\phi_{ref})} \cdot \ln(\phi) \tag{2.30}$$

Further it has been shown by Allard that Λ may be expressed in terms of macroscopic properties as:

$$\Lambda = \frac{1}{c_g} \sqrt{\frac{8\alpha_\infty \eta}{\phi \sigma^{static}}} \tag{2.31}$$

where c_g is dependent on the cross-sectional shape of the pores, for cylindrical geometries $c_g = 1$ [1]. Eq. (2.29) together with eq. (2.31) give

$$\sigma^{static} = \frac{8\alpha_\infty \eta}{1-(\rho^*/\rho_s)} \cdot \frac{16(\rho^*/\rho_s)^2}{d_s^2 c_g^2} \tag{2.32}$$

which when using a reference material may be expressed as

$$\sigma^{static} = \sigma_{ref}^{static} \left(\frac{\rho^*}{\rho_{ref}}\right)^2 \cdot \left(\frac{d_{ref}}{d_s}\right)^2 \cdot \frac{\alpha_\infty}{\alpha_{\infty ref}} \cdot \frac{\left(1-\frac{\rho_{ref}}{\rho_s}\right)}{\left(1-\frac{\rho^*}{\rho_s}\right)} \tag{2.33}$$

2.5 Aspects of optimization

Performing an optimization requires some type of objective function, $f(\mathbf{x})$, that provides a numerical value representing the qualities sought for. This objective function is dependent on one or more design variables, $\mathbf{x} = [x_1\, x_2 \cdots x_\mathrm{n}]$, limited by $\mathbf{x}_\mathrm{min} \leq \mathbf{x} \leq \mathbf{x}_\mathrm{max}$ and may also be subjected to different constraint functions, $g_\mathrm{i}(\mathbf{x})$. The optimization problem is often seen on the form

$$\begin{aligned} \min \quad & f(\mathbf{x}) \\ \text{subject to} \quad & g_1(\mathbf{x}) \leq 0 \\ & g_2(\mathbf{x}) \leq 0 \\ & \vdots \\ & g_\mathrm{M}(\mathbf{x}) \leq 0 \\ & \mathbf{x}_\mathrm{min} \leq \mathbf{x} \leq \mathbf{x}_\mathrm{max} \end{aligned} \tag{2.34}$$

Choosing a proper objective function and constraints is often more difficult than it may seem as in reality there are often many different objectives to meet which are dependent on the same or different design variables. In this work minimizing the acoustic discomfort or minimizing the mass are often the objectives used in practice. Alternative objectives may involve for example minimizing material cost, environmental impact, assembly time or fuel consumption and the minimum of one objective rarely coincide with the minima of the others. The problem may be handled by minimizing one objective while putting constraint on the others or by developing an objective function that incorporates several objectives into one single function, using for example some kind of weighted sum. There are many ways to construct an objective function and the task should not be taken lightly as the outcome of the optimization unavoidably will depend greatly on the choice of objective function and constraints.

In practise the optimization is often performed by some kind of algorithm. If the functions are differentiable and dependent on continuous design variables a gradient based algorithm is often suitable. Such algorithm has to be provided with information of the numerical values of the objective function, the gradient vector and possible parts of the Hessian matrix of that objective function with regard to $\mathbf{x}$, as well as

the numerical value of the constraint functions and possible the gradients and also the minimum and maximum values of the design variables. The algorithm will then, based on the input data, suggest new design parameters for which the cost function is calculated and so on in an iterative fashion until some kind of stop criterion is met. In practical applications are the objective function and/or the constraint functions often very complex and not uncommonly the result of some sort of computer simulation. This often requires the gradient and Hessian values to be calculated numerically, using for example finite differences, which increases the computational cost with every design variable used, and every iteration needed to find a minimum.

Another difficulty when using an optimization approach is that most objective functions are not convex, meaning that it may exist one or more local minima within the parameter range that are not the best solution. The best solution is instead referred to as the global minimum. This issue is most often handled by using several different starting point within the parameter range and then comparing the number of local minima and the value of the objective functions at those local minima.

Chapter 3

Studies of poro-elastic acoustic materials in multilayered structures

This work explores the possible effect of altering the microscopic properties of specific poro-elastic acoustic materials when assembled in multilayered acoustic or multifunctional panels. While the majority of the work concerns isotropic modelling the influence of anisotropic material properties and the angular orientation of those properties is also touched upon. The studies were conducted as numerical simulations using Biot theory and the, for this purpose, suitable FE-based numerical approach described in Chapter 2. The alterations of material properties were chosen by a gradient based optimizer [32, 33].

While optimizing the macroscopic porous material properties used in the Johnson-Champoux-Allard model may render some information concerning sought for combinations of material properties, it does however not provide any knowledge regarding what type of porous material to use or how to achieve such properties in any porous material in reality. Quite possible the resulting material would be physically impossible to realize, thus making such an optimization less useful in practice. By describing the poro-elastic acoustic material with its microscopic properties and thereafter estimate the corresponding macroscopic material parameters the resulting material may be, if not already existing, at least well described and physically possible to create. Hence the need for the previously described scaling laws which provide approximative correlations between microscopic and macroscopic parameters.

To examine the acoustic and dynamic behaviour of poro-elastic materials assembled in multilayered panels a number of different panels, containing either isotropic or anisotropic porous materials, have been numerically evaluated. The panels were exited by different types of force fields and the acoustic and dynamic properties needed to be expressed as an objective function or a constraint function in order to enable an optimization. Such a function may be chosen in a number of different ways and formulating a way to describe good and bad sound quality using a numerical quantitative

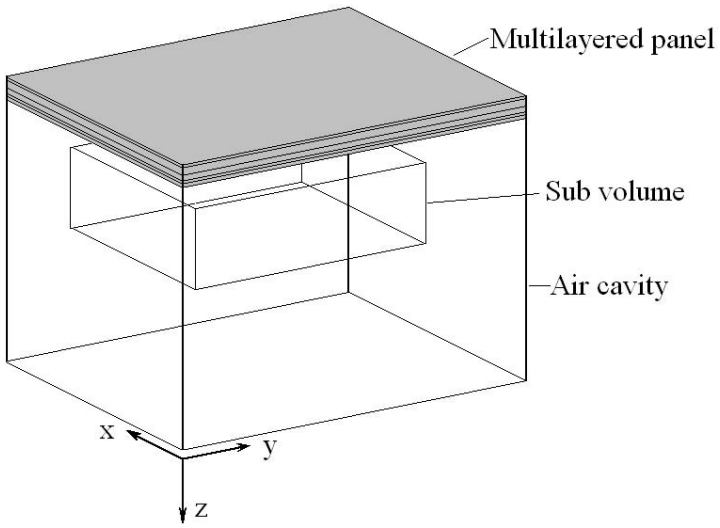

Figure 3.1: Schematic picture of multilayered panel and connected air cavity with subvolume.

value is not an easy task and represents a whole field of research in itself. In this work acoustic and dynamic measure was constructed as the acoustic response in a sub volume of an air cavity connected to the multilayered panel in question, fig. 3.1. The acoustic response was chosen to be the sound pressure level (SPL), inherently dependent on the different design parameters. The sound pressure square, p_f^2, for each evaluated frequency, f, is calculated as the average of the square sound pressure in a number, N, of discrete points in the chosen sub volume, eq. (3.2). This quantity was then multiplied with the frequency resolution, Δf_f, a frequency dependent weighting factor, C_f, divided with the reference sound pressure square, p_0^2, and summed over the entire frequency range, eq. (3.1), resulting in a total sound pressure level, SPL, which is then subject to minimization or maximization

$$\langle SPL \rangle_{\Omega_{\text{sub}}}^{C} = 10 \cdot \log \left(\frac{\sum_{f=f_1}^{f_{\max}} \left(p_f^2 \cdot \Delta f_f \cdot C_f \right)}{p_0^2} \right) \tag{3.1}$$

where

$$p_f^2 = \frac{1}{N} \sum_{n=1}^{N} p_{f_n}^2 \tag{3.2}$$

As the SPL in the air cavity was calculated for each frequency in the chosen frequency range the computational cost to evaluate eq. 3.1 may be quite substantial. In addition when the gradients are calculated using finite differences yet another evaluation of $\langle SPL \rangle_{\Omega_{\text{sub}}}^{C}$ is needed for each design variable. Therefore it is of great importance to,

within the optimization process, find a minimum with as few iterations as possible. The optimizer chosen here was an MMA (Method of Moving Asymptotes) based optimizer, and later on its refined globally convergent version [32, 33], as this optimizer performed well while using less iterations than the tested alternatives.

3.1 Adapting porous material parameters for improved acoustic performance

Initially a 2D-model was used to simulate a panel with seven layers, out of which one was microstructurally optimized, using an isotropic porous material model with the bulk density, ρ^*, and the strut thickness, d_s, as the design variables. The weighting factor in eq. 3.1 was set to correspond to either A-weighted or C-weighted SPL and two different open cell poro-elastic cellular foams were used, a polyurethane based foam, PU-foam, and a polyimide based foam, π-foam. Five different optimizations were executed: minimizing the SPL corresponding to A-weighting with constraint on the mass using PU-foam, minimizing the SPL corresponding to C-weighting with constraint on the mass using PU-foam, minimizing the SPL corresponding to C-weighting with constraint on the mass using *pi*-foam, and finally minimizing the mass using PU-foam and π-foam respectively, with constraints on the SPL corresponding to C-weighting. The SPL was evaluated for a frequency range 100 – 900 Hz. Also, constraints were put on the design variables to exclude results that were physically impossible.

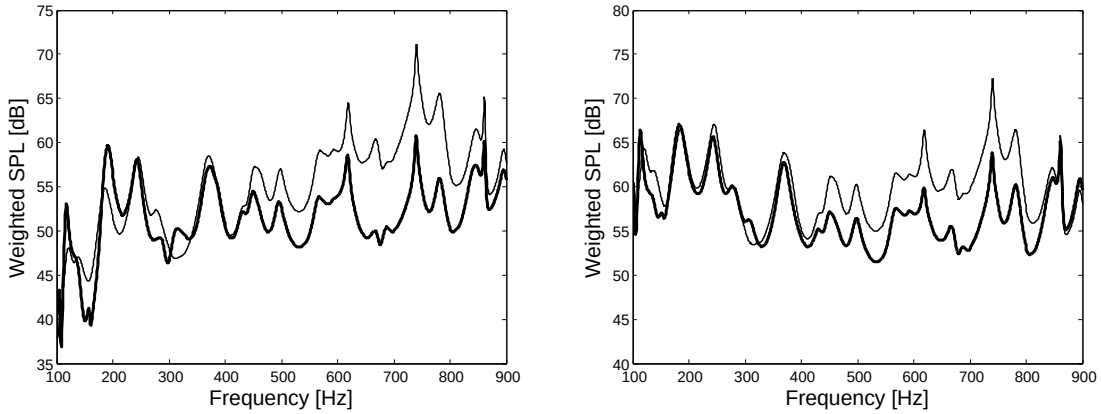

(a) A-weighted FRF

(b) C-weighted FRF

Figure 3.2: Frequency response function for optimal foam solution (thick solid) and suboptimal foam solution (thin solid), weighted with corresponding A-weighting (left figure) and C-weighting (right figure) respectively.

Although different starting points were used the final minimum remained the same, indicating that the objective functions were relatively convex for the parameter space and the frequency range chosen for these simulations. The resulting design parameters also show that the weighting function had a major impact on the outcome of the

optimization, using an A-weighted SPL the minimum was found at ρ^*=32.5 kg m^{-3} and d_s=14.8×10^{-6} m whereas the minimum was found at ρ^*=20.1 kg m^{-3} and d_s=15.5×10^{-6} m when a C-weighted SPL was used. Comparing the frequency response functions, FRFs, of the optimized panels with those of panels containing foam with suboptimal design parameters, also showed that the possibility of improvement in acoustic and dynamic behaviour was significant, see fig. 3.2

When comparing panels containing PU-foam and π-foam respectively, for C-weighted sound pressure optimized panels, the panel containing PU-foam performed slightly better. On the other hand, when minimizing the mass with constraints on C-weighted SPL the result was somewhat in favour of the panel containing π-foam.

The influence of anisotropy was examined using a 3D-model where a quadratic multilayered panel consisting of two aluminium face sheets separated by two layers of poro-elastic material, elastically bonded to the face sheet where the excitation was applied and separated by a thin air gap from the other aluminium face sheet. Two different varieties of the panel were considered: configuration A, containing an open cell orthotropic foam and configuration B, containing a transversely isotropic fibrous material. For both configurations, A and B respectively, both layers consisted of the same material type. The only variations introduced were the relative orientation of the material properties in each layer, which could rotate independently in different directions and thereby possibly achieving different overall dynamic properties considering the direction of excitation, see fig. 3.3.

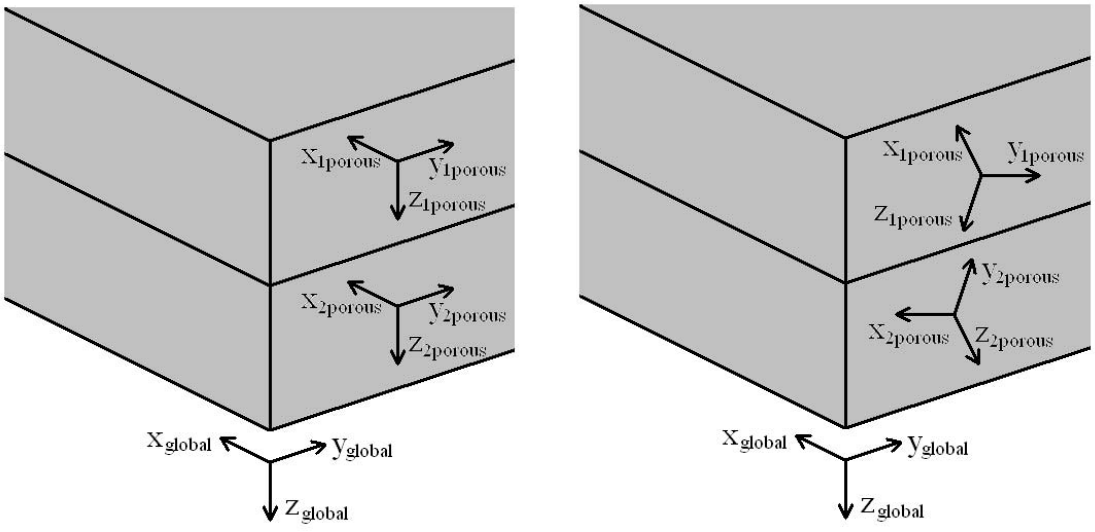

(a) Porous material orientation with [0 0 0]-rotation in both layers.

(b) Porous material orientation with different [α β γ]-rotation in layer 1 and layer 2.

Figure 3.3: Global and local co-ordinate axes and example of possible layer rotations of porous layer 1 and 2 in the panel used in the anisotropic simulation.

The anisotropy of the porous materials were described by and limited to the Hooke's matrix, the flow resistivity tensor and the tortuosity tensor. The objective function

was chosen as the unweighted SPL, eq. 3.1, and the design variables were the Euler angles describing a Z-Y-X fixed axis rotation. As the two porous layers could rotate independently of each other and rotation around the z-axis is redundant for transversely isotropic porous materials the number of design variables needed were six for configuration A and four for configuration B. Both minimizations and maximizations were performed for a number of different starting points.

While the different starting points resulted in more than one minimum and maximum the FRF of the different minima and maxima, although having different material property angles, showed great similarities and the differences in SPL between different minima were also less than 0.5 dB. The overall results show that the acoustic and dynamic properties of the panels were sensitive to angular changes of anisotropic porous materials. The difference between the best case found and the worst case found was 4.6 dB for configuration A and 4.7 dB for configuration B.

3.2 Combined structural and acoustic optimization – a multidisciplinary design tool

Historically, the handling of sound and vibration issues in engineering has taken place in the final stages of the design process when major parts of the structure is already fixed, or sometimes even later, when a noise, vibration and harshness (NVH) problem is already an inevitable fact. This approach may often create the need for after treatment of new lightweight designs, making them less weight optimized and more costly than originally expected. A design tool developed to handle both structural and acoustic issues at an early stage could hopefully make such expensive after treatment redundant. Yet another advantage would be if a design tool could take advantage of the small, but still existing, load bearing capabilities of poro-elastic acoustic materials as well as the naturally occurring acoustic damping properties of lightweight sandwich structures, all within one early design process. Part of the work was dedicated to this complex issue of developing an approach and a method of combining structural and acoustic optimization of multilayered panels within reasonable computational time compared to today's standard.

The starting point for this optimization concept was to replace a conventional car roof, fig. 3.4, with a multilayered panel containing both structural and acoustic porous materials. And while fulfilling the structural requirements, also be optimized considering mass as well as acoustic and dynamic properties.

The multilayered replacement was represented by a flat quarter model with symmetry boundary conditions applied through all layers along the symmetry edges. The inner perforated plate was also fixed in the x-, y- and z-direction along x=0 and y=0. Dynamic forces were applied in x-, y- and z-direction for a frequency range 100 – 500 Hz, fig. 3.5.

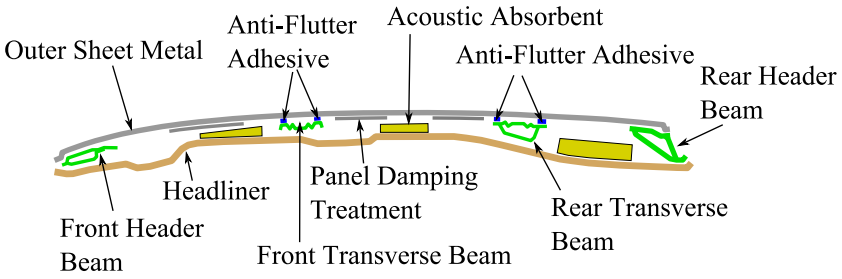

Figure 3.4: Schematic picture of conventional car roof.

As the car roof was represented by a flat panel in the numerical model the effects of the double curved surface of a normal car roof is omitted. Further it should be noted that symmetry boundary conditions preclude non-symmetric modes of vibration. Comparing the results directly with a conventional car roof may therefore be misguiding. However, the conceptual design methodologies presented are valid within their own premiss and may in the future be transferred to more complex panel shapes.

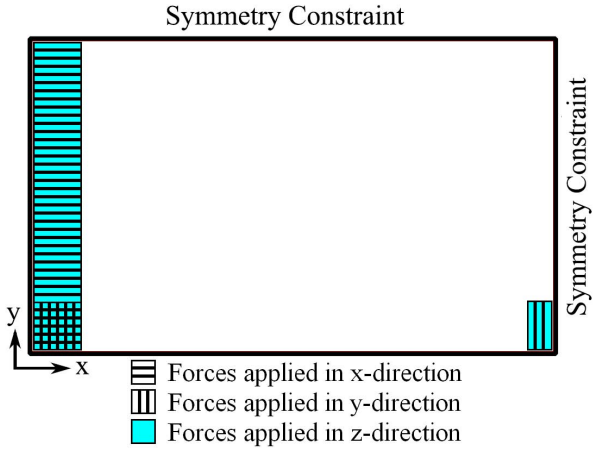

Figure 3.5: Dynamic forces applied to the CF Laminate.

The general design of the lightweight panel replacing the conventional car roof was an outer face sheet of carbon fibre (CF) reinforced epoxy composite laminate and an inner face sheet of perforated CSM (Chopped Strand Mat) GF (Glass Fibre) reinforced plastic. In between the two face sheets different combinations of structural and acoustic porous materials and, in certain configurations, air layers or air pockets were used. For computational reasons the optimization process was divided into different part which were executed in a sequential iterative manner.

Initially four different configurations were tested, where the structural and acoustic foam was divided into different layers, see fig. 3.6, except around the edges of the quarter model where the structural foam directly connected the inner and outer face sheets. Foam A was a PU-foam and foam B a π-foam.

The iterative process started with a structural mass optimization where three different load cases were applied, localised loading, distributed pressure, normal modes analysis,

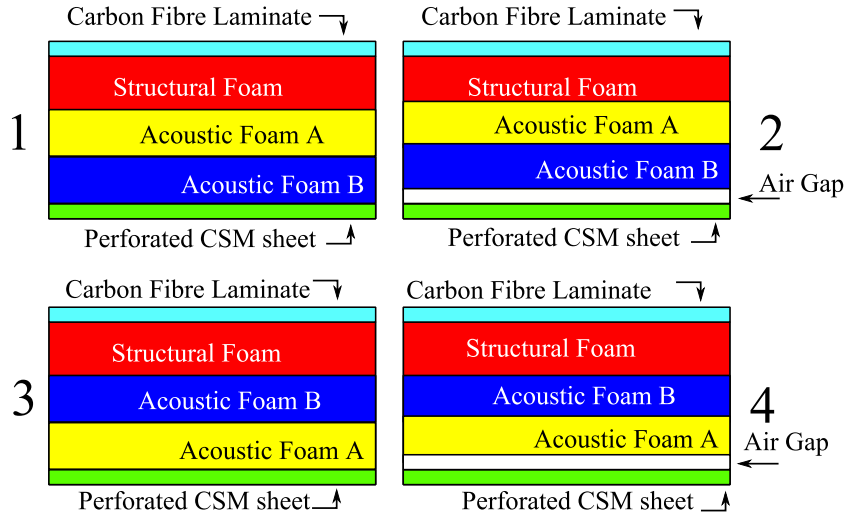

Figure 3.6: Stacking sequence of the different configurations.

using nine design variables and constraints on local and global stiffness so that the system did not exceed a given displacement, neither locally or globally, and so that the frequency of the first eigen mode of the panel would exceed a given minimum. Constraints were also put on the nine design variables. At this point general assumptions were made regarding the properties of the acoustic layers. Thereafter was an acoustic optimization performed, optimizing the relative strut length and the layer thicknesses of the two foam layers, with constraints on the total thickness. The results of the acoustic optimization were then given as input to a second iteration starting with structural optimization. Convergence was achieved after two to three iterations. The results are partly summarized in table 3.1.

		Configuration			
		1	2	3	4
Variable		PU-π	PU-π-air	π-PU	π-PU-air
ρ_{struct}	[kg/m^3]	134	128	143	141
ρ^*_{PU}	[kg/m^3]	38.6	138	138	138
t_{PU}	[mm]	23.0	48.0	47.2	41.5
ρ^*_{pi}	[kg/m^3]	9.31	1.48	2.46	3.86
t_{pi}	[mm]	27.0	1.00	2.46	4.59
Total Thickness	[mm]	79.1	78.7	78.7	75.8
Total Mass	[kg]	18.7	27.3	27.8	26.7
First Eigen Mode	[Hz]	71.8	46.9	64.7	47.0
SPL	[dB]	60.1	59.3	57.9	58.5

Table 3.1: Summary of final values of design variables and main results.

During the optimization process it became clear that the stacking sequence had a great influence on the acoustic response of the panel, especially for the configurations without air gap. Introducing an air gap also resulted in an unavoidably softer panel with a significantly lower first eigen mode. This was expected as the bounding of the core

material to the face sheets is a crucial part of having a structurally stiff low weight sandwich panel. In spite of the softness of acoustic foam its presence and coupling to the inner surface seems to be enough to prevent it from vibrating on its own, and also raising the overall stiffness.

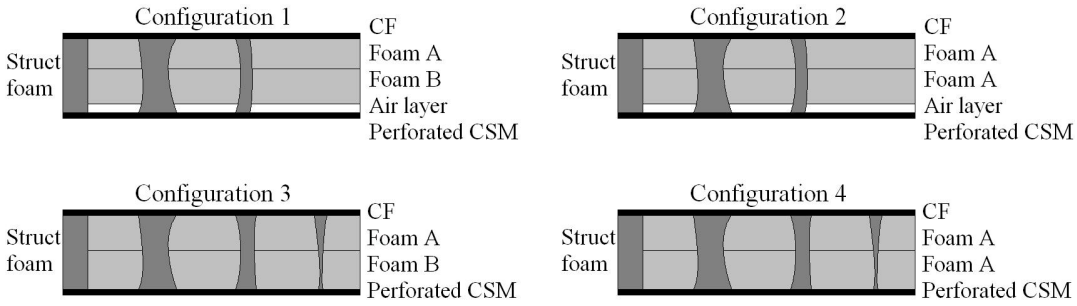

Figure 3.7: Conceptual visualization of the four different configurations. Note that the structural foam topology (dark grey) differs between the air gap and the non air gap configurations.

As a second step of this multidisciplinary design methodology the structural foam was no longer placed in a layer of its own but rather distributed in the core of the panel using topology optimization except along the edges of the panel where a frame of structural foam was used. The part of the core volume without structural foam was divided into two layers of acoustic foam. Four different configurations were set up in which two also an air gap was included, fig. 3.7. Foam A was a PU-foam and foam B a π-foam.

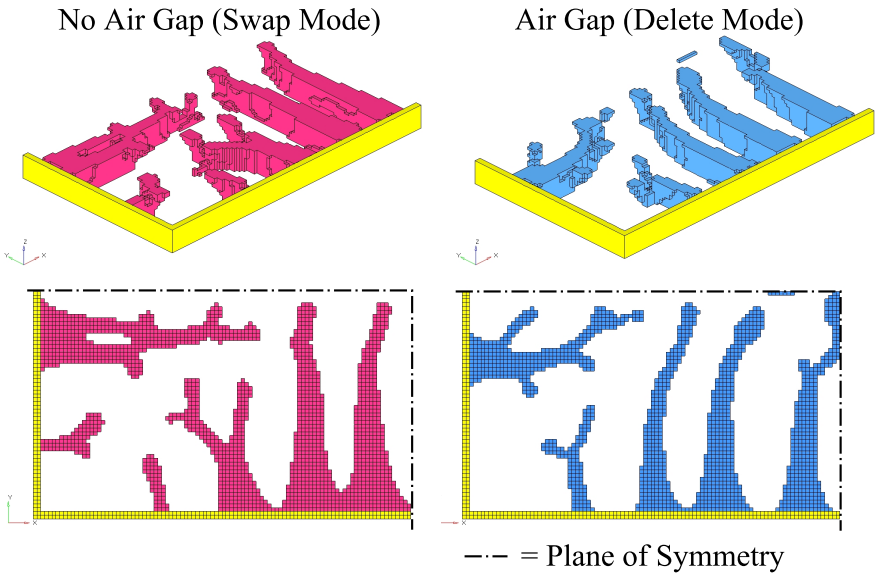

Figure 3.8: Final topology for structural foam in the 1/4 model. Left picture without air gap and right picture with air gap. The frame of fixed elements is also depicted.

This methodology started with a topology optimization using general foam parameters and four different load cases, localized load, distributed pressure, normal modes analysis and in-plane loading, with constraints on local and global stiffness so that the system did not exceed a given displacement, neither locally or globally, also the first eigen mode

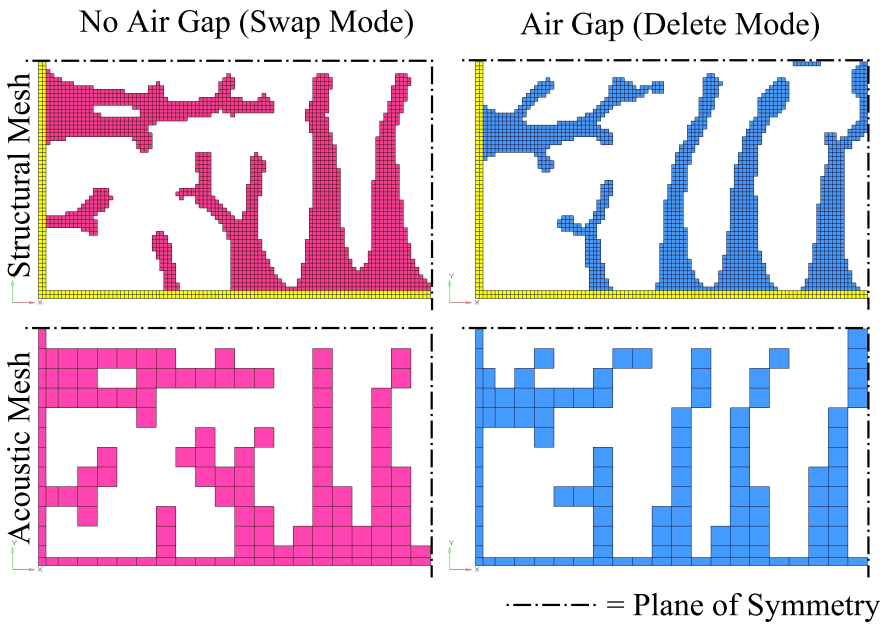

Figure 3.9: Comparison of stuctural (above) and acoustic (below) FE mashes of structural foam core material in the 1/4 model. Left picture without air gap and right picture with air gap. The frame of fixed elements is also depicted.

of the panel should exceed a given minimum frequency and finally a constraint were put on the in plane stability of the panel (buckling). This resulted in two basic structures, one for configurations with air gap and one for configurations without air gap, fig. 3.8. The next step was then the nine structural design variables and finally the four acoustic material parameters were optimized, the relative strut length and the layer thicknesses of the two foam layers. For computational reasons the acoustic model required an increase of element size compared to the structural optimization, see fig. 3.9. The results are partly summarized in table 3.2.

		Configuration			
		1	2	3	4
Variable		PU-π-air	PU-PU-air	PU-π	PU-PU
ρ_{struct}	[kg/m^3]	120	120	105	105
ρ^*_{layer1}	[kg/m^3]	36.3	13.5	6.80	5.01
t_{layer1}	[mm]	72.9	1.00	1.00	4.08
ρ^*_{layer2}	[kg/m^3]	5.29	138	1.96	27.9
t_{layer2}	[mm]	1.00	72.9	73.8	70.7
Total Thickness	[mm]	77.4	77.4	77.3	77.3
Total Mass	[kg]	18.2	31.6	14.0	17.1
SPL	[dB]	70.5	68.7	74.3	71.6

Table 3.2: Summary of final values of design variables and main results.

The results showed that the optimized acoustic foam gave an improved SPL in the air cavity, fig. 3.10. In one case, however, the improvement was combined with a quite severe mass penalty. Although configuration one and two had the same structural

properties the acoustic properties, solely influenced by the acoustic foam layers, were quite different. The acoustic response of configuration three and four also show that the acoustic foam combined with different choice of layer combinations as well as microscopic properties may give significant differences in acoustic signature, fig. 3.11.

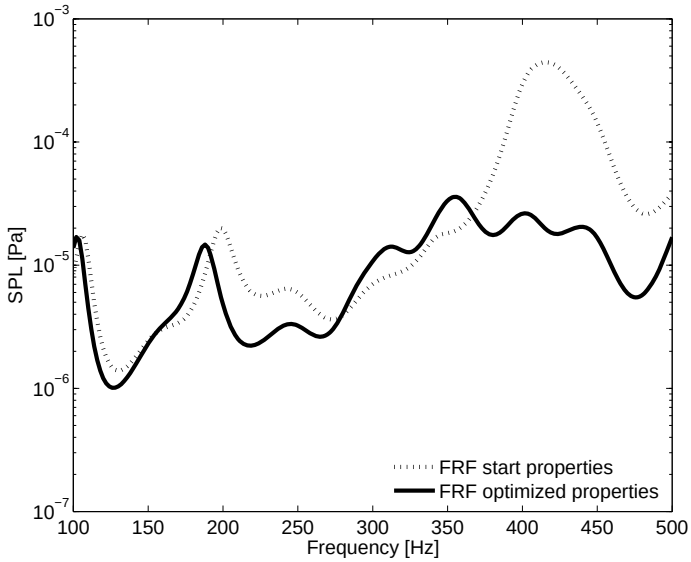

Figure 3.10: Frequency response function for the starting properties and optimized properties of configuration 1.

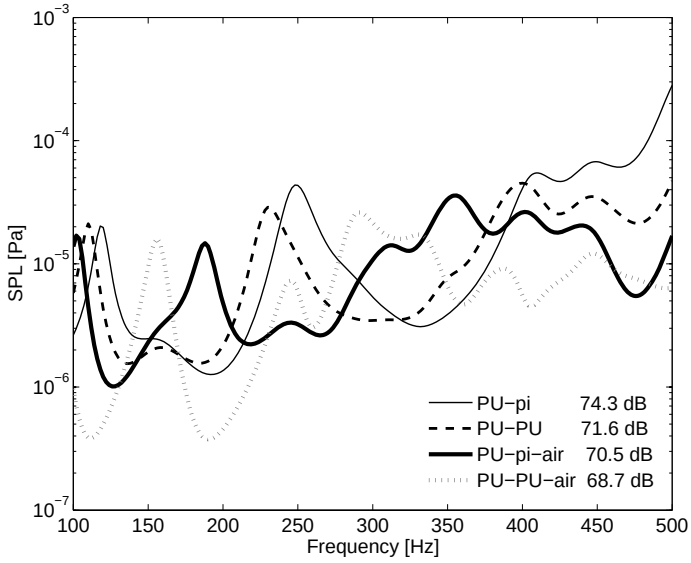

Figure 3.11: Frequency response functions of optimized properties for all configurations.

Chapter 4

Conclusions

The work presented here shows that small alterations of the microscopic geometrical material properties of open cell poro-elastic materials can cause differences of the macroscopic behaviour that is large enough to have a significant impact on the acoustic and dynamic response when assembled in multilayered panel configurations. For anisotropic poro-elastic materials the angular orientation of the macroscopic material properties in individual layers are shown to be important for the overall acoustic and dynamic behaviour of a multilayered panel. As both this and previous work have demonstrated the choice of acoustic poro-elastic materials, layer combinations and layer thicknesses are also of great importance when designing multilayered panels. These physical aspects imply that there are great potential to adapt multilayered structures to specific needs as well as to acoustic and dynamic circumstances.

While previously acoustic treatment has often been added late in the design process there are potentially some great advantages in combining structural and acoustic demands into multifunctional panel structures, as the sandwich panel already have several built-in acoustic benefits, such as fairly high damping, and the acoustic poro-elastic material, however comparably soft, may still contribute to the overall structural performance. However combining these two disciplines requires the development of new design tools, an extensive work of which a small part has been carried out in this thesis.

To efficiently find optimal or at least significantly improved material parameters an optimization approach has been implemented with a previously established finite element numerical modelling tool. The optimization approach is shown to be a fairly efficient and useful way to find such suitable material parameters. However, optimizing a panel for a certain wanted behaviour implicitly demands knowledge of what that behaviour is and how to express it as a numerical value dependent on the design variables. It should be stressed that a properly chosen objective function is crucial as it significantly affects the outcome of the optimization. Achieving a useful result is also dependent of quite detailed knowledge of the load cases and boundary conditions of the system.

Finally, the modelling approaches presented here have the ability of constituting a part of

a useful computer aided design tool, especially when developing lightweight multilayered panels. Such a design tool may be of great importance when striving for lighter and more energy efficient vehicle concepts in the future as it could help maintaining or even improving the NVH properties which are otherwise often penalized when reducing the weight of a structure.

4.1 Future work

A natural continuation of the initialized work on anisotropic poro-elastic material would be to develop computationally efficient scaling laws or other ways to connect microscopic and macroscopic properties for such materials. There is also room for improvement of the suggested scaling laws for isotropic materials. There is a general need for increased understanding of the physical behaviour of poro-elastic materials, especially when assembled in different structures as it may involve several different aspects such as pre-compression of the porous material and difficulties in assigning proper boundary conditions. Achieving such knowledge includes development of measurement techniques of the macroscopic material properties, the physical modelling of those properties and their connection to the geometrical microscopic properties, understanding and modelling of different damping phenomena as well as understanding and modelling of variations of the macroscopic material properties close to the boundaries of a poro-elastic material. For anisotropic poro-elastic materials this need is even greater as the understanding of anisotropic acoustic and dynamic phenomenas in such materials is today quite limited.

To better understand the complex coupled structural acoustic behaviour and to further extend the possibilities of designing mass and space efficient multifunctional panels is also highly sought after. Such knowledge must also be implemented in usable computationally efficient multidisciplinary design tools in order for it to truly make a difference in industrial production techniques.

Increasing the understanding and developing usable models in these areas may be a significant contribution to increase functionality and lower the environmental impact of vehicles and other structures in the future.

Chapter 5

Summary of papers

Paper I

Optimising open porous foam for acoustical and vibrational performance.

E. Lind Nordgren and P. Göransson

A computational method for optimizing microstructural properties of open cell porous foam assembled in multilayered acoustic panels is presented. The method uses previously established scaling techniques to link the microstructural properties to the classical Biot-Johnson-Champoux-Allard macroscopic parameters. This combined with Biot theory allows for calculations of an objective function and also its gradients by using finite differences and thereafter to access a gradient based optimizer. The outer surface of the panel was excited by three separate force fields and the acoustic properties of the panel were evaluated by calculating the sound pressure level for a frequency range 100 – 900 Hz in an air cavity attached to the panel. Different cost functions were tested and the results suggested that if alterations of the microscopic properties of the foam are made, the foam may be adapted to specific environmental conditions and thereby achieve improved acoustic behaviour as well as reduced weight. The choice of cost functions, as well as the chosen frequency range, was however greatly influencing the outcome of the optimization and must be chosen with care.

Paper II

Material Property Based Structural and Acoustic Optimization of a Multifunctional Vehicle Body Panel.

C. J. Cameron, E. Lind Nordgren, P. Wennhage and P. Göransson

A novel design approach involving combined structural and acoustic optimization is proposed that allows for a multilayered load bearing sandwich panel with integrated acoustic capabilities. The method is based on an iterative two-step optimization technique where a mass minimizing structural optimization is followed by an acoustic optimization. The outcome of the acoustic optimization was then used as a starting point for the next iteration beginning with structural optimization. Four different configurations were tested, two of which had an air gap included. Apart from the air gap the panels consisted of a thin carbon fibre laminate face sheet, one layer of structural closed cell polymer foam, two layers of lightweight open cell poro-elastic acoustic foam followed by the optional air gap and finally a thin perforated glass fibre reinforced inner face sheet. The structural as well as the acoustic optimization allowed for variation of the microscopic properties as well as variation of the layer thicknesses within certain boundary conditions. The acoustic response was evaluated for a frequency range 100 – 500 Hz by calculating the sound pressure level in an air cavity connected to the panel. Evaluating the resulting panels it was obvious that the presence or absence of an air gap, as well as the stacking sequence of the acoustic foam layers were of great importance for acoustic and dynamic properties while for the static structural properties the influence of the stacking sequence of the acoustic foam was small or insignificant. The results also indicated that there may be potential advantages of introducing acoustic absorbents in load bearing sandwich panels as the acoustic absorbers, in spite of their low stiffness, still contribute to the overall stiffness of the panel while also being able to improve dynamic and acoustic properties.

Paper III

A Design Method using Topology, Property, and Size Optimization to Balance Structural and Acoustic Performance of Sandwich Panels for Vehicle Applications.

C. J. Cameron, E. Lind Nordgren, P. Wennhage and P. Göransson

A combined structural and acoustic optimization process including topology optimization for load bearing panels is presented. Several different optimization stages were

used starting with a topology optimization to establish the most effective locations for load bearing material within the core of the panel. As a result the inner and outer surface of a panel were connected through a finger like framework of stiff, closed cell, structural foam. Thereafter was a mass optimization process used to tune the exact properties of the outer and inner face sheet as well as the structural foam. The remaining sandwich core volume, not occupied by structural foam was then filled with open cell poro-elastic acoustic materials divided into different layers. Four different configurations were tested, two of which had an air gap next to the inner surface and two had not. The acoustic response was evaluated for a frequency range 100 – 500 Hz by calculating the sound pressure level in an air cavity connected to the panel as the panel was excited by three different dynamic forces. Although the outer and inner surface of the panel were connected by stiff structural foam the results showed that the acoustic properties were still quite affected by small changes in the microstructure of the acoustic porous materials. The design methodology developed also showed a potential to combine and handle not only the intrinsic coupling but also the conflicts between the two physical mechanisms addressed, by offering a new approach to systematically deal with the combined structural and acoustic requirements.

Paper IV

Alignment of anisotropic poro-elastic layers - Sensitivity in vibroacoustic response due to angular orientation of anisotropic elastic and acoustic properties.

E. Lind Nordgren, P. Göransson and J.-F. Deü

A numerical experiment was performed to explore the influence of angular changes of anisotropic poro-elastic layers in multilayered acoustic panels. Two different materials were tested, one orthotropic open cell lightweight acoustic foam and one transversely isotropic fibrous material. The simulation set up consisted of two independent layers of the same porous material connected to an aluminium plate along one surface and separated from an identical aluminium plate through an air gap along the other surface. The sensitivity to angular changes of the porous layers was evaluated as an optimization problem where an objective function was both minimized and maximized in order to compare possible extremal points. The outer surface of each panel was excited by a unit force for a frequency range 100 – 700 Hz and the objective function was defined as the sound pressure level in an air cavity connected to the inner surface. The results showed that anisotropy of poro-elastic acoustic absorbers as well as their angular orientation both had significant influence in terms of acoustic properties of multlayered panels.

Chapter 6

Appendix

6.1 Notations in latin letters

Variable	
$b(\omega)$	viscous drag parameter
$B(\omega)$	frequency dependent function
c_g	pore shape dependent constant
C	solid frame Hooke's tensor
C^{ρ}	material dependent scaling constant for bulk density
C^{dl}	material dependent scaling constant for bulk Young's modulus
C^{E}	material dependent scaling constant for bulk Young's modulus
d	unjacketed compressibility compliance tensor
d_s	average strut thickness of solid frame
E_s	Young's modulus for solid frame material
E^*	Young's modulus for homogenized porous material
K_f	bulk modulus of fluid in the pores
K_s	bulk modulus of the solid frame material
l_s	average strut length of solid frame
p	acoustic pressure
Q	material tensor
R	material scalar
u^f	displacement vector of fluid
u^s	displacement vector of frame

6.2 Notations in greek letters

Greek letter	
α_∞	tortuosity
ε^s	solid frame strain tensor
η	fluid viscosity
θ^f	divergence of fluid displacement
Λ	viscous characteristic length
Λ'	thermal characteristic length
ν	Poisson's ratio
ρ_0	density of fluid
ρ_1	bulk density of solid frame
$\tilde{\rho}^{11}$	complex dynamic mass density for the solid phase
$\tilde{\rho}^{12}$	complex dynamic inertial coupling factor
$\tilde{\rho}^{22}$	complex dynamic mass density for the fluid phase
ρ_a	coupling factor modelled as added density
ρ_s	density of solid frame material
ρ^*	bulk density of solid frame
σ^f	Cauchy stress tensor for fluid
σ^s	Cauchy stress tensor for frame
σ^{static}	static flow resistivity of porous material
ϕ	porosity, volume fraction of open pore fluid content
ω	frequency

6.3 Material properties of reference materials

The Polyurethane foam (PU-foam) and Polyimide foam (π-foam) used as reference foam in this work had the following material properties.

Material property		PU-foam	π-foam
ρ_s	[kg m^{-3}]	1100	1400
E_s	[Pa]	$450 \cdot 10^6$	$1400 \cdot 10^6$
α_∞	[1]	1.17	1.17
ρ_0^*	[kg m^{-3}]	35.4	8
E_0	[Pa]	$164 \cdot 10^3$	$848 \cdot 10^3$
σ_0	[kg m^{-3} s^{-1}]	4500	$1000 \cdot 10^3$
Λ_0	[m]	$96.1 \cdot 10^{-6}$	$39 \cdot 10^{-6}$

Bibliography

[1] J.-F. Allard. *Propagation of sound in porous media: modelling sound absorbing materials.* Elsevier Applied Science, 1993.

[2] J.-F. Allard and Y. Champoux. New empirical equations for sound propagation in rigid frame fibrous materials. *J. Acoust. Soc. Am.*, 6(91):3346–3353, 1992.

[3] N. Atalla, M. A. Hamdi, and R. Panneton. Enhanced weak integral formulation for the mixed (u,p) poroelastic equations. *J. Acoust. Soc. Am.*, 109(6):3065–3068, 2001.

[4] N. Atalla, R. Panneton, and P. Debergue. A mixed displacement-pressure formulation for poroelastic materials. *J. Acoust. Soc. Am.*, 104(3):1444–1452, 1998.

[5] M. A. Biot. Theory of propagation of elastic waves in a fluid saturated porous solid. I. Low frequency range. *J. Acoust. Soc. Am.*, 28:168–178, 1956:1.

[6] M. A. Biot. Theory of deformation of a porous viscoelastic anisotropic solid. *J. Appl. Phys.*, 27:459–467, 1956:3.

[7] M. A. Biot. Mechanics of deformation and acoustic propagation in porous media. *J. Appl. Phys.*, 33(4):1482–1498, 1962.

[8] M. A. Biot and D. G. Willis. The elastic coefficients of the theory of consolidation. *J. Appl. Mech.*, 24:594–601, 1957.

[9] Y. Champoux and J.-F. Allard. Dynamic tortuosity and bulk modulus in air-saturated porous media. *J. Appl. Phys.*, 70(4):1975–1979, 1991.

[10] J. Comiti and M. Renaud. New model for determining mean structure parameters of fixed beds from pressure drop measurements. Application to beds packed with parallellepipedal particles. *Chemical Engineering Science*, 44(7):1539–1545, 1989.

[11] O. Doutres, N. Atalla, and K. Dong. Effect of the microstructure closed pore content on the acoustic behavior of polyurethane foams. *J. Appl. Phys.*, 110(6), 2011.

[12] K. Dovstam. Augmented Hooke's law in frequency domain. A three dimensional material damping formulation. *Int. J. Solids Structures*, 32(19):2835–2852, 1995.

[13] A. Geslain, O. Dazel, J.-P. Groby, S. Sahraoui, and W. Lauriks. Influence of static compression on mechanical parameters of acoustic foams. *J. Acoust. Soc. Am.*, 130(2):818–825, 2011.

[14] L. J. Gibson and M. F. Ashby. *Cellular solids — Structure and properties.* Cambridge University Press, second edition, 1997. First published by Pergamont Press Ltd., 1988.

[15] P. Göransson. Acoustic and vibrational damping in porous solids. *Phil. Trans. R. Soc. A*, 364:89–108, 2006.

[16] P. Göransson, R. Guastavino, and N.-E. Hörlin. Measurement and inverse estimation of 3d anisotropic flow resistivity for porous materials. *J. Sound Vib.*, 327(3-5):354–367, 2009.

[17] R. Guastavino and P. Göransson. A 3d displacement measurement methodology for anisotropic porous cellular foam materials. *Polymer Testing*, 26(6):711–719, 2007.

[18] N.-E. Hörlin. 3-D hierarchical hp-FEM applied to elasto-acoustic modelling of layered porous media. *J. Sound Vib.*, 285(4):341–363, 2005.

[19] N.-E. Hörlin and P. Göransson. Weak, anisotropic symmetric formulations of biot's equations for vibro-acoustic modelling of porous elastic materials. *Int. J. Numer. Meth. Engng*, 84(12):1519–1540, 2010.

[20] N.-E. Hörlin, M. Nordström, and P. Göransson. A 3-D hierarchical FE formulation of Biot's eguations for elasto-acoustic modelling of porous media. *J. Sound Vib.*, 254(4):633–652, 2001.

[21] W.-Y. Jang, A. M. Kraynik, and S. Kyriakides. On the microstructure of open-cell foams and its effect on elastic properties. *Int. J. Solids Structures*, 45(7-8):1845–1875, 2008.

[22] W.-Y. Jang, S. Kyriakides, and A. M. Kraynik. On the compressive strength of open-cell metal foams with kelvin and random cell structures. *Int. J. Solids Structures*, 47(21):2872–2883, 2010.

[23] D. L. Johnson, J. Koplik, and R. Dashen. Theory of dynamic permiability and tortuosity in fluid-saturated porous media. *J. Fluid Mech.*, 176:379–402, 1987.

[24] J. Åkerman and M. Höjer. How much transport can the climate stand?-sweden on a sustainable path in 2050. *Energy Policy*, 34(14):1944–1957, 2006.

[25] P. Khurana, L. Boeckx, W. Lauriks, P. Leclaire, O. Dazel, and J.-F. Allard. A description of transversely isotropic sound absorbing porous materials by transfer matrices. *J. Acoust. Soc. Am.*, 125(2):915–921, 2009.

[26] D. Lafarge, P. Lemarnier, J.-F. Allard, and V. Tarnow. Dynamic compressibility of air in porous structures at audible frequencies. *J. Acoust. Soc. Am*, 102(4):1995–2006, 1997.

[27] G. A. Lesieutre. Finite elements for dynamic modelling of uniaxial rods with frequency-dependent material properties. *Int. J. Solids Structures*, 28:1567–1579, 1992.

[28] M. Melon, E. Mariez, C. Ayrault, and S. Sahraoui. Acoustical and mechanical characterization of anisotropic open-cell foams. *J. Acoust. Soc. Am.*, 104(5):2622–2627, 1998.

[29] C. Perrot, F. Chevillotte, M. Tan Hoang, G. Bonnet, F.-X. Bécot, L. Gautron, and A. Duval. Microstructure, transport, and acoustic properties of open-cell foam samples: Experiments and three-dimensional numerical simulations. *J. Appl. Phys.*, 111(1), 2012.

[30] C. Perrot, R. Panneton, and X. Olny. From microstructure to acoustic behaviour of porous materials. *Canadian Acoustics - Acoustique Canadienne*, 32(3):18–19, 2004.

[31] S. Sahraoui, E. Mariez, and M. Etchessahar. Linear elastic properties of anisotropic open-cell foams. *J. Acoust. Soc. Am.*, 110(1):635–637, 2001.

[32] K. Svanberg. The method of moving asymptotes — a new method for structural optimization. *Int. J. Numer. Meth. Engng*, 24:359–373, 1987.

[33] K. Svanberg. A class of globally convergent optimization methods based on conservative convex separable approximations. *SIAM Journal on Optimization*, 12(2):555–573, 2002.

[34] C. Zwikker and C. Kosten. *Sound absorbing materials.*, chapter II and III. Elsevier Publishing Company, Amsterdam, 1949.

Part II

Appended papers